BOUNDARY LAYER OF NON-NEWTONIAN FLUIDS OBEYING A RHEOLOGICAL POWER LAW FOR ARBITRARY PRESSURE GRADIENTS

A. Sh. Dorfman and V. K. Vishnevskii

UDC 532.517.2

The equations of the boundary layer associated with non-Newtonian fluids obeying a rheological power law are integrated by a semiintegral method based on the simultaneous solution of the linearized equation of motion and the integral relationship.

A method of calculating the properties of a boundary layer based on the simultaneous solution of the equations of motion (linearized by means of a suitable set of profiles) and the integral relationship was developed in [1-3]. This method may be called the semiintegral or parametric-linearization method; it gives a highly accurate solution at all points except in the region close to the break-off point, as may be confirmed by a calculation of the second approximation [2] and comparison with numerical solutions. If it is necessary to increase the accuracy, the second and subsequent approximations may be calculated. In addition to this, the semiintegral method provides simple relationships between the fundamental characteristics of the boundary layer and the velocity distribution outside the layer as well as the longitudinal derivatives of this.

In this paper the semiintegral method is employed to integrate the equations of the boundary layer of non-Newtonian fluids obeying a rheological power law [4]

$$\overline{\overline{\tau}}=K\left(\frac{1}{2}J_2\right)^{\frac{n-1}{2}}\overline{\overline{e}}. \tag{1}$$

Formulas will be obtained for the velocity distribution in the boundary layer and the frictional forces at the wall for an arbitrary velocity distribution outside the layer. Tables of coefficients will be given for calculating the friction associated with different values of the index n. By way of example we shall consider flow around a circular cylinder. We shall derive the frictional stress distribution on the surface of the cylinder for various values of n, and shall calculate the second approximation for this case. We shall establish the relationship between the position of the break-off point on the cylinder and the index n of the non-Newtonian behavior of the fluid.

The problem of the flow of non-Newtonian fluids obeying a power law for arbitrary pressure gradients has been solved by a number of authors using integration and other approximate methods [4]. However, the accuracy of these methods falls sharply for values of n appreciably deviating from unity [4, 5]. The problem was solved in [5] in the form of Blasius series. However, the slow convergence of the series meant that these could only be used at short distances from the critical point of the cylinder.

The equations of the boundary layer in fluids obeying a law of type (1) take the following form [4] (in future we shall use dimensionless variables)

$$u\frac{\partial u}{\partial x}+v\frac{\partial u}{\partial y}=U\frac{dU}{dx}+\frac{\partial}{\partial y}\left|\frac{\partial u}{\partial y}\right|^n, \tag{2}$$

$$\frac{\partial u}{\partial x}+\frac{\partial v}{\partial y}=0, \tag{3}$$

$$y=0,\ u=v=0;\ y=\infty,\ u=U(x).$$

Institute of Technical Heat Physics, Academy of Sciences of the Ukrainian SSR, Kiev. Translated from Inzhenerno-Fizicheskii Zhurnal, Vol. 20, No. 3, pp. 398-404, March, 1971. Original article submitted March 24, 1970.

Treating n as arbitrary, let us introduce variables analogous to the variables of Hertler [6] in the case of a Newtonian fluid

$$\Phi = \int_0^x U^{2n-1}(x)dx, \quad \varphi = \frac{\psi}{[n(n+1)\Phi]^{\frac{1}{n+1}}}. \tag{4}$$

In order to obtain an equation of the Prandtl–Mises type instead of (2), we take (4) as independent variables. Since the continuity equation is satisfied on introducing the current function, after certain transformations we may replace the system (2) by the following equation

$$(n+1)\Phi\frac{\partial Z}{\partial \Phi} - \varphi\frac{\partial Z}{\partial \varphi} - \frac{u}{U}\left|\frac{u}{U}\cdot\frac{\partial}{\partial\varphi}\left(\frac{u}{U}\right)\right|^{n-1}\frac{\partial^2 Z}{\partial\varphi^2} = 0; \tag{5}$$

$$\varphi = 0, \ Z = U^2(\Phi); \ \varphi = \infty, \ Z = 0. \tag{6}$$

In order to linearize this equation we use automodel solutions obtained for a power-type velocity distribution $U = cx^m$ in the external flow, as in the case of the Newtonian fluid [1, 3]. Denoting the automodel velocity distribution by $\alpha(\varphi, m, n)$ and using it to calculate the coefficient attached to the second derivative in Eq. (5), we obtain the following linear equation

$$(n+1)\Phi\frac{\partial Z}{\partial \Phi} - \varphi\frac{\partial Z}{\partial \varphi} - \alpha\left|\alpha\frac{d\alpha}{d\varphi}\right|^{n-1}\frac{\partial^2 Z}{d\varphi^2} = 0. \tag{7}$$

For boundary conditions (6) the solution of this equation may be expressed by the series

$$Z = \sum_{k=0}^{\infty} A_k S_k, \tag{8}$$

where

$$S_0 = U^2, \ S_1 = \Phi(U^2)' \ldots \ S_k = \Phi^k(U^2)^{(k)} \ldots$$

are functions of the longitudinal coordinate x calculated from the known U(x) (' signifies differentiation with respect to Φ). The coefficients $A_k(\varphi, m, n)$ are determined by the ordinary differential equations obtained on substituting the series (8) into (7) ($\cdot$ signifies differentiation with respect to φ):

$$\begin{gathered} \alpha|\alpha\dot{\alpha}|^{n-1}\ddot{A}_k + \varphi\dot{A}_k - (n+1)kA_k = (n+1)A_{k-1}, \\ A_0(0) = 1, \ A_k(0) = A_k(\infty) = 0. \end{gathered} \tag{9}$$

Using the series (8) we find the frictional stress at the wall. Referring this to the quantity $\rho[U_\infty^{3n}K/\rho L^n]^{1/(n+1)}$, we obtain

$$\tau_w = \Phi^{-\frac{n}{n+1}}\left[\sum_{k=0}^{\infty} a_k S_k\right]^n. \tag{10}$$

The coefficients $a_k = -2^{-1}[n(n+1)]^{-[1/(n+1)]}\dot{A}_k(0, m, n)$ are determined by integrating Eq. (9) in the same way as in the case of a Newtonian fluid [3]. The values of the first five coefficients a_k are given in Table 1.

For a given n the coefficients of series (8) and (10) depend on the parameter m determining the automodel profile chosen for linearizing the initial equation (5). The value of this parameter may be determined from the integral relationship or some other integration condition. The choice of integration condition has little effect on the results of the calculation. It is most convenient [3] to use a condition based on equating the energy-loss thicknesses δ^{***} corresponding to the profile found from Eq. (8) and the automodel profile respectively. This condition leads to the following relation [3]:

$$\begin{gathered} \int_0^\infty\left[\left(\frac{u}{U}\right)^2 - \alpha^2\right]d\varphi = \sum_{k=0}^{\infty} D_k S_k = 0; \\ D_0 = \int_0^\infty (A_0 + \alpha^2 - 1)\,d\varphi; \ D_k = \int_0^\infty A_k d\varphi. \end{gathered} \tag{11}$$

If, as in [3], we approximate the $D_k = D_k(D_0)$ relationships by linear equations and solve the equation thus obtained from (11), we may deduce a formula giving the relation between D_0 and the specified functions $S_k(x)$:

TABLE 1. Values of the Coefficients a_k

n	0,4	0,6	0,8	1	1,2	1,4	1,6	1,8	2
D_0	0	0	0	0	0	0	0	0	0
a_0	0,349	0,325	0,324	0,332	0,345	0,360	0,374	0,389	0,403
a_1	0,937	0,813	0,771	0,757	0,754	0,760	0,769	0,779	0,793
$-a_2$	0,135	0,113	0,103	0,099	0,096	0,095	0,094	0,093	0,093
$10a_3$	0,283	0,231	0,208	0,194	0,185	0,178	0,175	0,172	0,170
$-10a_4$	0,054	0,043	0,039	0,035	0,032	0,031	0,030	0,029	0,028
D_0	1,710	0,675	0,341	0,187	0,122	0,088	0,066	0,054	0,044
a_0	0,280	0,276	0,293	0,313	0,334	0,355	0,374	0,390	0,406
a_1	0,966	0,770	0,669	0,616	0,587	0,570	0,558	0,553	0,548
$-a_2$	0,138	0,109	0,091	0,081	0,074	0,070	0,067	0,065	0,063
$10a_3$	0,293	0,222	0,184	0,157	0,140	0,130	0,120	0,115	0,110
$-10a_4$	0,056	0,042	0,032	0,028	0,025	0,022	0,020	0,018	0,017
D_0	4,11	1,440	0,580	0,296	0,180	0,124	0,091	0,070	0,058
a_0	0,182	0,232	0,274	0,305	0,330	0,352	0,374	0,391	0,408
a_1	1,013	0,748	0,628	0,564	0,513	0,514	0,505	0,500	0,493
$-a_2$	0,144	0,107	0,086	0,074	0,067	0,063	0,059	0,057	0,056
$10a_3$	0,306	0,217	0,174	0,144	0,125	0,117	0,106	0,100	0,094
$-10a_4$	0,058	0,040	0,031	0,026	0,022	0,020	0,018	0,017	0,015

TABLE 2. Values of the Coefficients b_k and d_k

n	0,4	0,6	0,8	1	1,2	1,4	1,6	1,8	2
$-b_1$	1,165	0,643	0,424	0,310	0,239	0,195	0,167	0,145	0,133
b_2	0,439	0,228	0,144	0,100	0,074	0,058	0,048	0,041	0,037
$-10b_3$	1,213	0,604	0,368	0,249	0,178	0,135	0,110	0,091	0,081
$10b_4$	0,263	0,127	0,076	0,050	0,035	0,026	0,021	0,018	0,015
d_1	−0,521	−0,394	−0,166	0,046	0,207	0,336	0,435	0,519	0,591
d_2	0,213	0,163	0,062	−0,027	−0,088	−0,130	−0,167	−0,200	−0,236
$10d_3$	−0,609	−0,475	−0,172	0,090	0,275	0,356	0,440	0,514	0,572
$10d_4$	0,135	0,107	0,026	−0,026	−0,056	−0,081	−0,098	−0,110	−0,121

$$D_0 = \frac{\sum_{k=1}^{\infty} b_k S_k}{S_0 + \sum_{k=1}^{\infty} d_k S_k}. \tag{12}$$

The values of the first four coefficients b_k and d_k are given in Table 2 for different values of n.

Practical calculations are extremely simple and are carried out in the following way. From the specified velocity distribution U(x) outside the layer and Eq. (4) we find the values of $\Phi(x)$ and then the function $S_k(x)$. We determine the coefficients b_k and d_k from Table 2 for a given n, then use (12) to determine the values of the parameter $D_0(x)$, and turn to Table 1. For each value of n this table gives the first five coefficients a_k for three values of the parameter D_0, embracing the range of D_0 values required from the practical point of view. The $a_k = a_k(D_0)$ dependence is very weak, so that for intermediate values of D_0 the coefficients a_k may be determined by linear interpolation. This gives sufficient data to calculate the frictional stress at the wall from Eq. (10).

If necessary the velocity distribution in the layer (in the x, φ plane) may be determined from (8). The coefficients A_k are also tabulated. The transition to the real x, y plane and the calculation of the characteristic layer thicknesses are carried out in the same way as for a Newtonian fluid [3].

The results may be refined, if necessary, by taking the foregoing as a first approximation and then calculating the next approximations. Usually the second approximation differs little from the first, even in the break-off region, and consideration may be limited to the second. In the rest of the flow the first approximation is usually sufficient, since it is almost exactly repeated by the next approximations.

In order to calculate the next approximations we turn (as in [2]) to Eq. (5), considering that the first term in this equation and the coefficient of the second derivative are calculated from the results of the

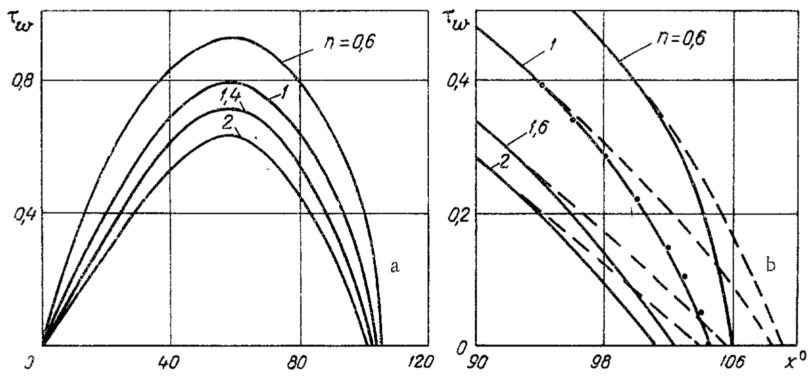

Fig. 1. Variation in the dimensionless frictional stress on the surface of a circular cylinder (a) and calculated values of the dimensionless frictional stress in the break-away region (b) in relation to n.

previous approximation. Then Eq. (5) may be considered as an ordinary linear equation in the function Z to be determined in the next approximation. Integrating Eq. (5) under these conditions and satisfying the boundary conditions (6), we obtain

$$Z_{i+1}=U^2+I_i-\frac{H_i}{H_i(\infty)}[U^2+I_i(\infty)], \tag{13}$$

where

$$H_i=\int_0^{\varphi} e^{-F_i}d\varphi,\ I_i=\int_0^{\varphi} e^{-F_i}\int_0^{\varphi}\frac{(n+1)\Phi}{f_i}\cdot\frac{\partial Z_i}{\partial\Phi}e^{F_i}d\varphi d\varphi;$$
$$F_i=\int_0^{\varphi}\frac{\varphi d\varphi}{f_i};\ f_i=\left(\frac{u}{U}\right)_i\left|\frac{1}{2U^2}\cdot\frac{\partial Z_i}{\partial\varphi}\right|^{n-1}. \tag{14}$$

$H_i(\infty)$, $I_i(\infty)$ are the values of the integrals (14) at $\varphi\to\infty$.

Making use of Eq. (13) it is not difficult to find the frictional stress at the wall in the (i + 1)-th approximation:

$$\tau_{w_{i+1}}=[n(n+1)\Phi]^{-\frac{n}{n+1}}\left[\frac{U^2+I_i(\infty)}{2H_i(\infty)}\right]^n. \tag{15}$$

It follows from the resultant relationships that the calculation of the next approximations reduces essentially to the calculation of the integrals (14). For the second approximation the quantities Z, u/U, and the corresponding derivatives are determined by means of the series (8), and for the next approximations by means of Eq. (13).

The integrand defining I in Eq. (14) increases infinitely as $\varphi\to 0$, and in the equation defining F it becomes indeterminate. Expanding these expressions in series around $\varphi = 0$, it may be shown that the integrand in F and the integral itself vanish at $\varphi = 0$, while the integrand in I increases without limit as $\varphi^{-1/2}$. Close to $\varphi = 0$ I may be expressed by the following series:

$$I=\frac{2^{3/2}(n+1)U^{2n-1}}{3[n(n+1)\Phi]^{\frac{2n-1}{2(n+1)}}\cdot\tau_w^{\frac{2n-1}{2n}}}\left[S_1\varphi^{3/2}-\frac{\varphi^{5/2}}{5(n+1)}\sum_{k=1}^{\infty}b_kS_k+\ldots\right],$$

where $b_k = 2n^{1/(n+1)}(n+1)^{(n+2)/(n+1)}(a_{k-1}+ka_k)$. This series enables us to determine the value of I for a certain φ_0 close to zero (in our present calculations $\varphi_0 = 0.005$). Subsequent calculation proceeds numerically.

Figures 1a and b show the calculated frictional forces at the wall of a circular cylinder for a sinusoidal velocity distribution at the outer boundary of the boundary layer: U = sin x. The broken lines show the results of a calculation based on Eq. (10); the continuous lines represent the second approximation. In addition to this, the points in Fig. 1b represent the data obtained for a Newtonian fluid (n = 1) in [7] by

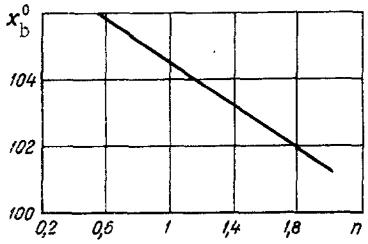

Fig. 2. Dependence of the central angle x_b^0 on the index n.

numerical integration of the boundary-layer equations, these being given for the sake of comparison.

We see from the results presented that a calculation based on Eq. (10) agrees with the results of the second approximation for all n and everywhere except in the region close to the break-away point. Close to this point series (8) and (10) diverge for $n \neq 1$. Nevertheless, the use of four terms with $n > 1$ and five with $n < 1$ in series (10) yields quite good results even in this region (Fig. 1b). The values of the central angle $x°$ defining the position of the break-away point found in the first and second approximations differ by only 3-4° for all values of n. This is no greater than the differences attributable to approximate methods of calculation (such as integration methods) even in the case of a Newtonian fluid, for which the errors are well known [4, 5] to be much smaller than in the case of $n \neq 1$.

We may judge the accuracy of the results obtained from the extent to which the second and first approximations agree, and also from the comparison with numerical-integration data presented in Fig. 1b, from which it follows that for $n = 1$ the two results practically coincide.

Thus the proposed method of calculation ensures a reasonably high accuracy in the first approximation (semiintegral method) at every point except in the region close to the break-away point, at which the second approximation is essential in order to produce an accuracy of the same order.

We see from Fig. 1a that, as the index n representing the non-Newtonian behavior of the fluid diminishes, the frictional stress at the wall of the cylinder increases. The break-away point then moves downward along the flow. The dependence of the central angle x_b° defining the position of the break-away point on the index n is extremely weak and almost linear (Fig. 2).

The very slight dependence of the position of the break-away point on the index supports the contention of earlier authors [8] to the effect that the mechanism underlying the viscous-elastic behavior of the fluid provides an explanation for the observed protraction of the break-away region when a pseudo-plastic fluid passes around a cylinder.

In conclusion, we may note that the proposed method of calculation may be used for integrating the equations of motion even for rheological laws more complicated than ordinary power laws. In order to linearize the original equation in this case we may use not only automodel solutions but also any other family of functions containing parameters and satisfying the corresponding conditions, for example, the families used in the construction of integration methods.

NOTATION

x, y	are the Cartesian coordinates;
u, v	are the components of the velocity vector along the coordinate axes;
U	is the velocity of the external flow;
ψ	is the current function;
$Z = U^2 - u^2$	is the auxiliary variable;
$\bar{\bar{\tau}}$	is the stress tensor;
$\bar{\bar{e}}$	is the tensor of deformation (shear) rates;
K	is the consistency index of the fluid;
n	is the index representing the non-Newtonian behavior of the fluid;
m	is the index in the power law of the external velocity distribution;
τ_w	is the stress at the wall;
J	is the second invariant of the tensor of deformation rates [4].

As scales for the dimensionless quantities we take: for x, the characteristic dimensions of the body L; for y, $L/\mathrm{Re}^{1/(n+1)}$, $\mathrm{Re} = (U_\infty^{2-n} L^n)/(K/\rho)$ the generalized Reynolds number; for u, U, the velocity a long way from the body U_∞;

$$v — \frac{U_\infty}{\mathrm{Re}^{\frac{1}{n+1}}};\quad \psi — \left[\frac{KLU_\infty^{2n-1}}{\rho}\right]^{\frac{1}{n+1}};\quad \tau_w — \rho\left[\frac{U_\infty^{3n}K}{L^n\rho}\right]^{\frac{1}{n+1}}.$$

LITERATURE CITED

1. A. Sh. Dorfman, Teplofiz. Vys. Temp., 5 (1967).
2. A. Sh. Dorfman, Abstracts of Contributions to the Third All-Union Congress on Theoretical and Applied Mechanics [in Russian], Nauka, Moscow (1968).
3. A. Sh. Dorfman and V. K. Vishnevskii, Prikl. Mekhan., 5, 9 (1969).
4. Z. L. Shul'man and B. M. Berkovskii, Boundary Layer of Non-Newtonian Fluids [in Russian], Nauka i Tekhnika, Minsk (1966).
5. Calvin I. Wolf and Albin A. Szewczyk, Proc. Third Internat. Heat Transfer Conf., Chicago, 111, 1966, Vol. 1, Amer. Inst. Chem. Engrs., New York N. 4 (1966), pp. 388-397.
6. P. G. Loitsyanskii, Laminar Boundary Layer [in Russian], Moscow (1962).
7. R. M. Terrill, Phil. Trans. Roy. Soc., 253, No. 1022, 55-100 (1960).
8. A. V. Lykov, Z. L. Shul'man, and B. I. Puris, Inzh.-Fiz. Zh., 14, No. 1 (1968).